Environmental Science & Technology

pubs.acs.org/est

Article

# Updated Reaction Pathway for Dichloramine Decomposition: Formation of Reactive Nitrogen Species and *N*-Nitrosodimethylamine

Huong T. Pham, David G. Wahman, and Julian L. Fairey*

Cite This: *Environ. Sci. Technol.* 2021, 55, 1740−1749

Read Online

ACCESS | Metrics & More | Article Recommendations | Supporting Information

**ABSTRACT:** The *N*-nitrosodimethylamine (NDMA) formation pathway in chloraminated drinking water remains unresolved. In pH 7−10 waters amended with 10 $\mu$M total dimethylamine and 800 $\mu$eq $Cl_2 \cdot L^{-1}$ dichloramine ($NHCl_2$), NDMA, nitrous oxide ($N_2O$), dissolved oxygen (DO), $NHCl_2$, and monochloramine ($NH_2Cl$) were kinetically quantified. $NHCl_2$, $N_2O$, and DO profiles indicated that reactive nitrogen species (RNS) formed during $NHCl_2$ decomposition, including nitroxyl/nitroxyl anion ($HNO/NO^-$) and peroxynitrous acid/peroxynitrite anion ($ONOOH/ONOO^-$). Experiments with uric acid (a $ONOOH/ONOO^-$ scavenger) implicated $ONOOH/ONOO^-$ as a central node for NDMA formation, which were further supported by the concomitant *N*-nitrosodimethylamine formation. A kinetic model accurately simulated $NHCl_2$, $NH_2Cl$, NDMA, and DO concentrations and included (1) the unified model of chloramine chemistry revised with HNO as a direct product of $NHCl_2$ hydrolysis; (2) $HNO/NO^-$ then reacting with (i) HNO to form $N_2O$, (ii) DO to form $ONOOH/ONOO^-$, or (iii) $NHCl_2$ or $NH_2Cl$ to form nitrogen gas; and (3) NDMA formation via $ONOOH/ONOO^-$ or their decomposition products reacting with (i) dimethylamine (DMA) and/or (ii) chlorinated unsymmetrical dimethylhydrazine (UDMH-Cl), the product of $NHCl_2$ and DMA. Overall, updated $NHCl_2$ decomposition pathways are proposed, yielding (1) RNS via $NHCl_2 \rightarrow HNO/NO^- \xrightarrow{O_2} ONOOH/ONOO^-$ and (2) NDMA via $ONOOH/ONOO^- \xrightarrow{\text{UDMH−Cl or DMA}}$ NDMA.

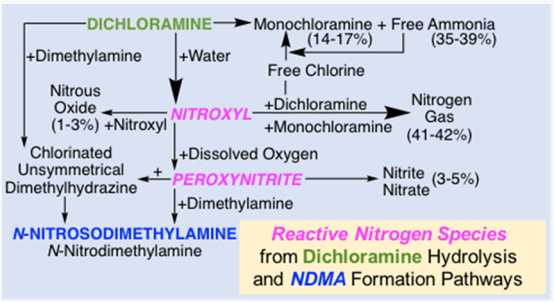


## INTRODUCTION

Chloramines are commonly used drinking water disinfectants in the United States.[1] While chloramination is associated with a decreased formation of regulated trihalomethanes and haloacetic acids, *N*-nitrosodimethylamine (NDMA) is a concern[2] given its formation at toxicologically relevant levels.[3] Some NDMA precursors are composed of secondary amines such as dimethylamine (DMA, $(CH_3)_2NH$)[4] as well as tertiary amines and quaternary ammonium compounds with DMA functional groups. These precursors include pharmaceuticals and personal-care products,[5] veterinary antibiotics,[6] anion exchange resins,[7] and unidentified components of pipeline materials.[8] In the conversion of DMA to NDMA, the nitrogen and oxygen in the added NO group have been attributed to chloramines[9] and dissolved oxygen (DO), respectively.[10−12]

Early studies with DMA as a model precursor postulated a two-step NDMA formation pathway in which monochloramine ($NH_2Cl$) and DMA reacted to form unsymmetrical dimethylhydrazine (UDMH), followed by a $NH_2Cl$ and UDMH reaction to form NDMA.[13,14] Schreiber and Mitch[10] cast doubt on this pathway by (i) showing that NDMA yields with $NH_2Cl$ and DMA were about 100 times greater than those with $NH_2Cl$ and UDMH and (ii) noting that the rate constant for UDMH formation[15] (0.081 $M^{-1} \cdot s^{-1}$) was about 100 times lower than needed (6.4 $M^{-1} \cdot s^{-1}$) to simulate their NDMA data.[13] This led to a revision and replacement of the NDMA−chloramine formation pathway[10] in which dichloramine ($NHCl_2$) was proposed as the primary reactant. This reaction pathway from Schreiber and Mitch[10] (SM) combines (i) 14 reactions from the unified (UF) model of chloramine chemistry[16] (Table S1, U1−U14) with (ii) 8 reactions that culminate in NDMA formation (Table S2, P1−P8) and associated acid−base chemistry (Table S3), referred to herein as the UF + SM model. This model is shown as Pathway A1 of Scheme 1 where, for clarity, only UF model reactions U3−U9 and NDMA formation reactions P5, P7, and P8 are presented. For NDMA formation, the first step is a reaction between $NHCl_2$ and DMA (P5) to form chlorinated unsymmetrical dimethylhydrazine (UDMH-Cl).

Received: September 25, 2020
Revised: December 23, 2020
Accepted: January 6, 2021
Published: January 15, 2021

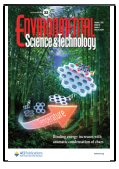







https://dx.doi.org/10.1021/acs.est.0c06456
*Environ. Sci. Technol.* 2021, 55, 1740−1749

**Scheme 1. NDMA Formation Stemming from $NHCl_2$ Decomposition in the Presence of DMA; See Table S1 (U1−U14) for UF Model Reactions**[a]

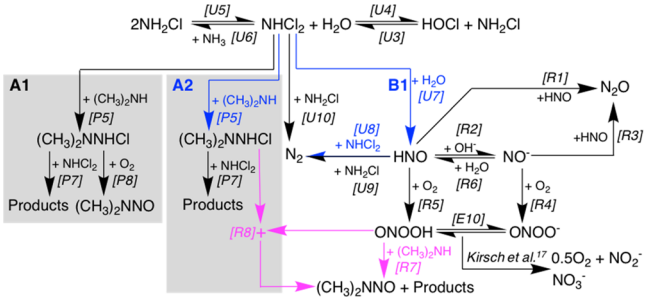


[a]**A1**: currently accepted $NHCl_2$−DMA reaction pathway represented by the UF + SM model;[10] see Table S2 for P1−P8 of the UF + SM model (replaced with A2 in the UF + RNS model). **B1**: proposed RNS scheme for $NHCl_2$ hydrolysis to HNO and subsequent formation of $N_2O$, ONOOH, and other products; see Tables S3 and S4 for the relevant equilibrium reactions and principal RNS model reactions, respectively. In the presence of DMA (R7), ONOOH (shown) and/or radicals formed from ONOOH/$ONOO^-$ decomposition (not shown) react with DMA to form NDMA. **A2**: proposed replacement of A1 in which ONOOH (shown) and/or radicals formed from ONOOH/$ONOO^-$ decomposition (not shown) react with UDMH-Cl to form NDMA. The UF + RNS model is composed of A2 and B1, the latter of which includes the 117 reactions in the ONOOH/$ONOO^-$ model of Kirsch et al.[17] with only the principal end products shown for simplicity. Reactions *[U#]*, *[P#]*, *[E#]*, and *[R#]* correspond to those listed in Tables S1−S4, respectively. Blue arrows and text denote the previously published reactions for which their rate constants were modified to fit the $NH_2Cl$, $NHCl_2$, DO, and NDMA kinetic data at pH 7−10 (see Table S9), and magenta arrows and text denote the new reactions and rate constants added to the UF + RNS model to fit these same data (see Table 1).

Next, UDMH-Cl reacts with DO to form NDMA (P8) or with $NHCl_2$ to form other products (P7). To curb NDMA formation, Pathway A1 emphasizes minimizing the $NHCl_2$ concentration[18] or removing and/or transforming DMA-like precursors.[19] However, P8 (UDMH-Cl + DO) is spin-forbidden and DO consumption was not previously kinetically validated,[10] prompting others to investigate other potential reaction pathways. Subsequent studies have found that NDMA yields from $NHCl_2$ and $NH_2Cl$ were dependent on the pH and precursor type. For example, in waters containing ranitidine, a high-yielding NDMA precursor containing a DMA functional group, NDMA yields at pH 8 were lower with $NHCl_2$ (ca. 47% yield) compared to $NH_2Cl$ (ca. 80% yield).[12] However, at pH 7, Huang et al.[20] found greater NDMA with $NHCl_2$ compared to $NH_2Cl$ with four *N,N*-dimethyl-*α*-arylamine precursors, including ranitidine. They computationally rationalized the contrary findings, attributing these to high $NHCl_2$ doses. Selbes et al.[21] found that $NH_2Cl$ preferentially reacted with precursors containing electron-withdrawing groups and $NHCl_2$ with precursors containing electron-donating groups.

Radical species in chloramine systems may also be relevant in NDMA formation. Spahr et al.[11] studied $NH_2Cl$ and ranitidine reaction kinetics at pH 8 and showed that radical scavengers (e.g., ABTS and Trolox) shut down NDMA formation, concluding that aminyl radicals (from $NH_2Cl$ oxidation of organic amines) and *N*-peroxyl radicals (from aminyl radicals reacting with DO) were part of the NDMA formation pathway. The hypothesized source of the radical was an electron transfer reaction of an amine with $NH_2Cl$ but was not demonstrated experimentally.

A long-standing unknown in the UF model that remained in the UF + SM model is the identity of the reactive intermediate (*I*) from $NHCl_2$ hydrolysis[16] (Table S1, U7). *I* has been hypothesized to be the reactive nitrogen species (RNS) nitroxyl (HNO),[22] but this has not been experimentally proven. HNO and its conjugate base, nitroxyl anion ($NO^-$), exist in a slow equilibrium because of the spin-forbidden oxygen transition from singlet state HNO to triplet state $NO^-$.[23] HNO/$NO^-$ are difficult to measure kinetically because they are short lived and unlikely to accumulate. However, HNO/$NO^-$ may react with HNO to form $N_2O$,[24] a stable end product, via R1 and R2 → R3 (see Scheme 1). Real-time $N_2O$ measurements can be made nondestructively using a $N_2O$ microelectrode;[25] therefore, $N_2O$ kinetic measurements would serve as a total nitroxyl (HNO plus $NO^-$) marker. In competition with $N_2O$ formation, DO may react in a pH-dependent manner with HNO or $NO^-$[26,27] via R5 and R2 → R4 (see Scheme 1) to form peroxynitrous acid/peroxynitrite anion (ONOOH/$ONOO^-$), which are also RNS. A microelectrode can be used to measure DO in real time,[11] and DO consumption would support HNO/$NO^-$ and ONOOH/$ONOO^-$ formation.

Once formed, ONOOH/$ONOO^-$ are unstable and known to decompose through a complex series of 117 reactions[17] to nitrite ($NO_2^-$) and nitrate ($NO_3^-$), which would both further serve as markers for ONOOH/$ONOO^-$ formation. With DMA present and competing with $NO_2^-$ and $NO_3^-$ formation, ONOOH/$ONOO^-$ may directly react with DMA or decompose to radical species that may react with DMA, forming NDMA and another suspected carcinogen, *N*-nitrodimethylamine (DMNO).[28,29] Uric acid is a known scavenger of ONOOH/$ONOO^-$ and its decomposition products,[30] including the free radicals $NO_2^{\bullet}$ and $CO_3^{\bullet-}$ that form by rapid decay of $ONOOCO_2^-$ and $O_2NOCO_2^-$, which are short-lived intermediates generated by the reaction of ONOOH/$ONOO^-$ with $CO_2$.[31] While uric acid is non-selective and can also scavenge reactive oxygen species such as hydroxyl radical and superoxide radical, Schreiber and Mitch[10] ruled out these species in the NDMA formation pathway through scavenging experiments with superoxide dismutase and *tert*-butanol (see Supporting Information S0.2 for details). Experiments with uric acid would allow for the evaluation of ONOOH/$ONOO^-$ (i) presence from $NHCl_2$ decomposition and (ii) importance in NDMA formation. Taken together, identifying *I* and understanding its fate during $NHCl_2$ decomposition may lead to an updated pathway for RNS and NDMA formation during $NHCl_2$ decomposition and/or a revised interpretation of the UF + SM model.

Based on the previous discussion, the objective of the current study was to evaluate revisions to the chemistry of $NHCl_2$ decomposition and associated NDMA formation with DMA present. To accomplish this, Pathway A1 was first evaluated through kinetic model simulations to assess the accuracy of NDMA formation kinetics in the UF + SM model at pH 7−10. Next, experiments (pH 7−10) were completed with and without 10 μM total DMA (TOTDMA, DMA plus dimethylammonium cation, $DMAH^+$) and 800 μeq $Cl_2 \cdot L^{-1}$ $NHCl_2$, measuring $NH_2Cl$, $NHCl_2$, $N_2O$, DO, and NDMA kinetically and $NO_2^-$, $NO_3^-$, and DMNO at 4 h. $NH_2Cl$, $NHCl_2$, and $N_2O$ data allowed the evaluation of the hypothesis


https://dx.doi.org/10.1021/acs.est.0c06456
Environ. Sci. Technol. 2021, 55, 1740−1749

that $I$ is HNO during $NHCl_2$ decomposition, and DO, $NO_2^-$, $NO_3^-$, and NDMA data allowed the evaluation of ONOOH/$ONOO^-$ formation and its potential relevance in NDMA formation. Furthermore, under drinking water conditions, DMNO most likely forms through a reaction of DMA with radicals that form during ONOOH/$ONOO^-$ decomposition.[17,32] Therefore, DMNO formation would further support a pathway containing ONOOH/$ONOO^-$. Additional experiments with uric acid, an ONOOH/$ONOO^-$ scavenger,[30] allowed the evaluation of ONOOH/$ONOO^-$ formation and its importance in NDMA formation. Concurrently with the kinetic experiments, a kinetic model was used to evaluate proposed revisions to $NHCl_2$ decomposition and NDMA formation chemistry, including the addition of HNO/$NO^-$, DO, and ONOOH/$ONOO^-$. Overall, the current study's objectives were to advance fundamental chloramine chemistry by evaluating the identity of $I$ during $NHCl_2$ decomposition, evaluate a pathway for RNS formation and propagation through DO consumption, and demonstrate the formation of toxicologically relevant end products such as NDMA through RNS-mediated pathways.

## MATERIALS AND METHODS

The following are detailed in the Supporting Information (SI): (i) reagent preparation and washing procedures (Supporting Information S1.1); (ii) chloramine preparation (Supporting Information S1.2); and (iii) chloramine (Supporting Information S1.3), $NO_2^-$ and $NO_3^-$ (Supporting Information S1.4), and NDMA and DMNO (Supporting Information S1.5) quantification. This section's remainder details the kinetic experiments, analytical techniques, and kinetic parameter estimation methodology.

**Chloramine Formation/Quenching, TOTDMA Addition, and NDMA/DMNO Extraction.** $NH_2Cl$ stock solutions were freshly prepared before each experiment[33] at ca. 4 mM to make $NHCl_2$ stock solutions as detailed in the Supporting Information (see S1.2). $NHCl_2$ stock solutions were made by decreasing the pH of the $NH_2Cl$ stock solutions to 3.7−4.0 with 4 N $H_2SO_4$ and aging for 45 to 60 min until all the $NH_2Cl$ was transformed to $NHCl_2$. Because $NHCl_2$ formation consumes protons, $H_2SO_4$ was added throughout the aging process to maintain the pH between 3.7 and 4.0.

$NHCl_2$ concentrations were quantified (Shimadzu UV 2450 spectrophotometer) following Schreiber and Mitch[18] by deconvoluting the 245 and 295 nm absorbance spectra. Within 15 min of complete conversion to $NHCl_2$, the $NHCl_2$ solutions were diluted to 0.4 mM $NHCl_2$ (800 $\mu$eq $Cl_2 \cdot L^{-1}$) with pH-adjusted buffer to the desired pH, which was time zero. For the experiments in which NDMA was measured, this buffer also contained TOTDMA.

The starting experiment concentrations were 40 mM for the phosphate (pH 7 and 8), borate (pH 9), or carbonate (pH 10) buffers and 10 $\mu$M for TOTDMA (pH 7−10). The initial TOTDMA and $NHCl_2$ concentrations were twice those used by Schreiber and Mitch,[10] which were done to exceed the detection limits for $N_2O$ formation and DO consumption at pH 7 and prolong the temporally changing periods at pH 8 and 9.

Following the desired reaction times (0.25, 0.5, 1.0, 1.5, 2.0, 2.5, 3.0, 3.5, and 4.0 h), waters were analyzed for $NHCl_2$; $NH_2Cl$; and, following the quenching of chloramine species, NDMA. DMNO was measured at 4 h only. For NDMA and DMNO, 10 mL aliquots were quenched for chloramines using 0.5 g of a dry quenching mix (1.8 g ascorbic acid, 1 g $KH_2PO_4$, and 39 g $Na_2HPO_4$) and shaken vigorously to ensure complete dissolution within a few seconds, minimizing localized concentration gradients.[10,12,34,35] This quenching mix acted as a pH buffer and salting out agent to improve the recoveries of NDMA and DMNO. Next, 1 mL of 100 $\mu g \cdot L^{-1}$ $d_6$-NDMA was added and samples were immediately extracted with dichloromethane (10:1 water/dichloromethane volume ratio) using a back-and-forth shaker table at high speed for 15 min. Following a 5-min quiescent settling period, dichloromethane was decanted with a Pasteur pipette and stored for NDMA and DMNO analysis.

**$N_2O$ and DO Microelectrode Measurements.** $N_2O$ and DO were measured using microelectrodes from Unisense that have manufacturer-reported response times of less than 45 and 10 s, respectively, and were calibrated before each experiment. Per the manufacturer's recommendation, $N_2O$ standards were made from dilutions of $N_2O$ saturated solution and had a 1.0 $\mu$M-N limit of quantification that produced signal-to-noise ratios greater than 10 for all experiments. The DO sensor used a two-point calibration: (i) atmospheric air saturated water and (ii) zero DO condition, achieved by scavenging DO with 0.1 M sodium ascorbate in 0.1 M NaOH.

**Kinetic Parameter Estimation Methodology.** To estimate parameters and their standard errors, the secant parameter estimation function in AQUASIM[36] was configured to minimize the weighted residual sum of squares (WRSS) between the measured and simulated results using the square of the measured value as the weight, resulting in a dimensionless WRSS.[25] This procedure was used to prevent greater concentrations from biasing the parameter estimates.[37]

## RESULTS AND DISCUSSION

**Preliminary Kinetic Evaluation of the UF + SM Model (Pathway A1).** Pathway A1 was originally developed and validated from end-point (e.g., 2 h reaction) NDMA measurements but was not validated with detailed kinetic measurements (pH 7−10) of reactants (e.g., DO or $NHCl_2$), intermediates (e.g., UDMH-Cl), or products other than NDMA.[10] If incomplete or not robust, viewing NDMA formation as Pathway A1 may not only limit the development of NDMA control strategies but fail to account for the production of RNS in chloramine systems and formation of RNS-mediated end products of human health concern.[28] The Supporting Information (see S2.1 and Figures S1 and S2) contains a detailed discussion of Pathway A1 kinetics that revealed two results subsequently questioned by the current experimental work: (1) DO consumption during $NHCl_2$ decomposition was nominal and only occurs in the presence of TOTDMA, and (2) at pH 9 and 10, NDMA formation continues after complete $NHCl_2$ decomposition.

**Applicability of the UF Model for Chloramine Profiles.** Under the conditions of the current experiments (decomposition of ca. 800 $\mu$eq $Cl_2 \cdot L^{-1}$ $NHCl_2$ at pH 7−10 with and without 10 $\mu$M TOTDMA addition), the UF model reactions control chloramine concentrations in Scheme 1. As detailed in the Supporting Information (S1.3 and S2.2), the UF model accurately simulated time-course profiles of total chlorine (Figure S3), and $NH_2Cl$ and $NHCl_2$ (Figures S4 and S5c,d). The slight mismatch of $NH_2Cl$ at pH 10 (Figure S4d) was not surprising because the original UF model[38,39] was validated at pH 6−9. These results illustrated the applicability


https://dx.doi.org/10.1021/acs.est.0c06456
Environ. Sci. Technol. 2021, 55, 1740−1749

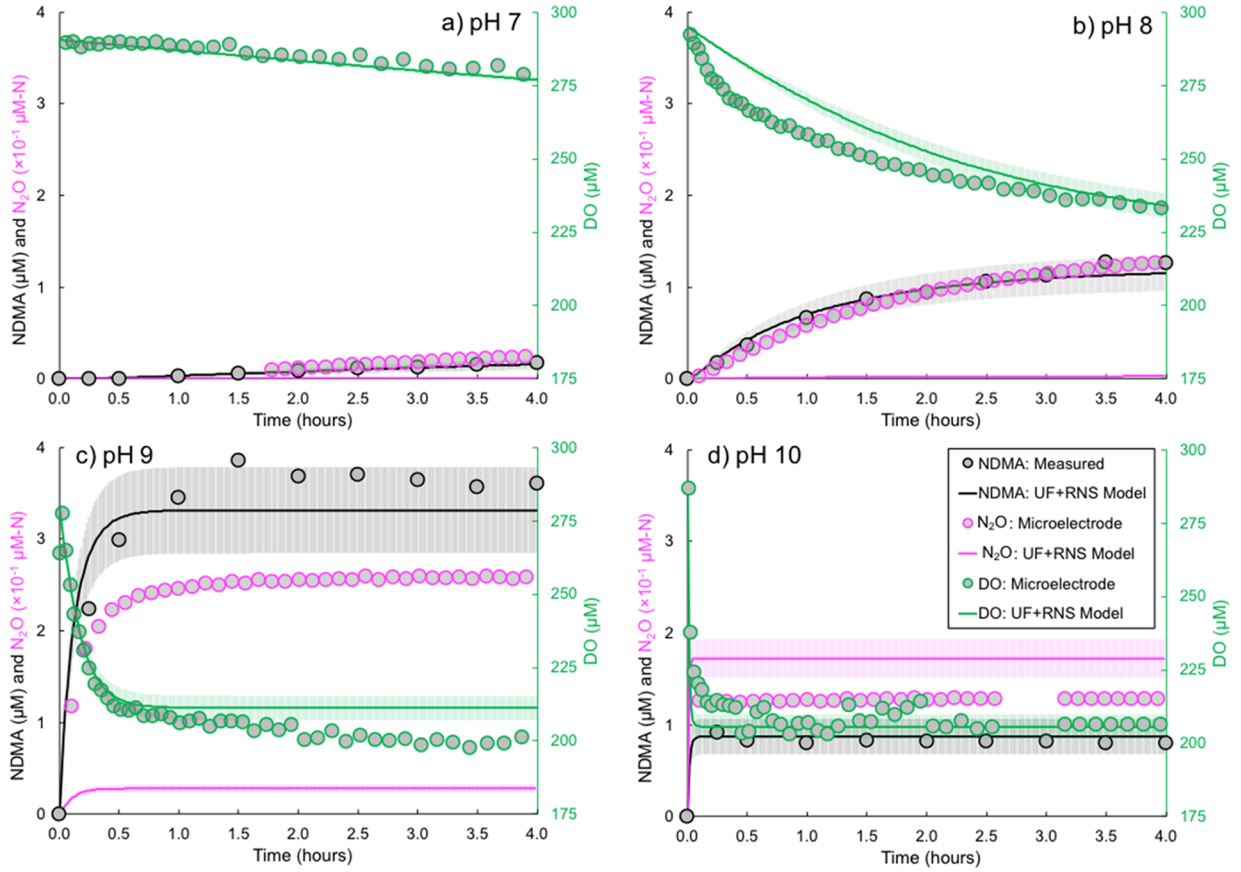


**Figure 1.** NDMA (black, primary *y* axis), $N_2O$ (magenta, primary *y* axis), and DO (green, secondary *y* axis) profiles in waters dosed with ca. 800 $\mu$eq $Cl_2 \cdot L^{-1}$ $NHCl_2$ and containing 10 $\mu$M TOTDMA buffered at pH (a) 7, (b) 8, (c) 9, and (d) 10. Points are measured values, lines are UF + RNS model simulations, and shaded areas are simulations encompassing 1 standard error in the estimated parameters (see Table 1). Table S9 contains the weighted residual sum of squares (WRSS) and the corresponding average weighted residual sum of squares (AWRSS) for data sets used in parameter estimation for the UF + RNS model (e.g., NDMA and DO). In addition, Table S10 contains the WRSS and AWRSS for the $N_2O$ data sets to provide an indication of how well the UF + RNS model simulated these data, which were not used during parameter estimation. Notes: $N_2O$ data were divided by 10 for scaling purposes (e.g., at pH 10, $N_2O$ stabilized at about 13 $\mu$M-N), and the limit of quantitation was 1 $\mu$M-N, which corresponded to a signal-to-noise ratio greater than 10; at pH 10, the gap in DO and $N_2O$ microelectrode data between 2.6 and 3.2 h was due to a lost computer connection.

of the UF model to simulate chloramine concentrations under the selected conditions in this study.

**Limitations of NDMA Simulations with the UF + SM Model (Pathway A1).** NDMA formation was measured kinetically in waters containing 10 $\mu$M TOTDMA and dosed with ca. 800 $\mu$eq $Cl_2 \cdot L^{-1}$ $NHCl_2$ at pH 7−10. Figure S6a (see Supporting Information S2.3) shows that the measured NDMA profiles at pH 7 and 8 were adequately simulated by the UF + SM model over the 4 h experiment. However, deficiencies in the UF + SM model were apparent at pH 9 and 10 (Figure S6b). At pH 9, the UF + SM model underpredicted the measured NDMA formation throughout the 4 h test by a factor of about 2.5. At pH 10, the UF + SM model underpredicted NDMA formation during the first hour, an indication that the underlying reaction kinetics were not robust. The measured NDMA profile was fully developed by the first sampling point at 0.25 h, whereas the UF + SM model simulated the increasing NDMA formation through ca. 2.0 h. These deficiencies along with the collected experimental data motivated the assessment of two additional pathways in Scheme 1 that are subsequently discussed: (1) Pathway B1 and (2) Pathway A2 as a replacement for Pathway A1.

**Proposed Pathways B1 and A2.** Pathway B1 (see Scheme 1) combines (i) the UF model (Table S1), assuming HNO as *I* in U7-U9, and (ii) reactions involving DO, HNO/$NO^-$, and other relevant RNS (Table S4, Supporting Information S2.4). RNS formation is initiated by $NHCl_2$ hydrolysis to HNO (U7) and $NO^-$ (U7 → R2). HNO/$NO^-$ may then react with (i) $NH_2Cl$ or $NHCl_2$ to form nitrogen gas ($N_2$) via U8−U10, which is expected to be the major end product in the UF model;[40] (ii) HNO to form $N_2O$ via R1 and/or R2 → R3 as a minor end product relative to $N_2$; or (iii) DO to form $ONOOH/ONOO^-$ via R4 and/or R2 → R5, which subsequently may react with DMA to form NDMA via R7. Otherwise, $ONOOH/ONOO^-$ decomposition results in $NO_2^-$ and $NO_3^-$ formation[17] as other minor end products relative to $N_2$. Pathway A2 revises Pathway A1, which included the spin-forbidden incorporation of DO to form NDMA (P8). In the proposed Pathway A2, NDMA is formed through a reaction with ONOOH (R8, see Scheme 1), which is pH-dependent because the $pK_a$ of 6.8 for $ONOOH/ONOO^-$ (see Table S3) is relevant between pH 7 and 10; the $pK_a$ for UDMH-Cl was estimated as 1.5,[41] and thus, its concentration is not affected by the acid−base speciation between pH 7 and 10. Experimental data and the associated kinetic modeling


https://dx.doi.org/10.1021/acs.est.0c06456
Environ. Sci. Technol. 2021, 55, 1740−1749

were subsequently used to evaluate the proposed Pathways B1 and A2.

**$N_2O$ Formation from $NHCl_2$ Decomposition.** To initiate Pathway B1, $NHCl_2$ hydrolysis (Scheme 1, U7) is hypothesized to form HNO. Subsequently, $N_2O$ may form from HNO (R1) or $NO^-$ (R2 → R3).[24] Because $N_2O$ is a stable end product, its detection serves as a $HNO/NO^-$ formation marker and would support Pathway B1.[42] Experiments were conducted with ca. 800 $\mu$eq $Cl_2 \cdot L^{-1}$ $NHCl_2$ and 10 $\mu$M TOTDMA at pH 7−10. Figure 1 shows that $N_2O$ formed at pH 7−10 with pH-dependent kinetics and yields, and Figure S7 (see Supporting Information S2.5) shows that these $N_2O$ profiles inversely tracked $NHCl_2$ decomposition. The $N_2O$ profiles, therefore, qualitatively support $HNO/NO^-$ formation from $NHCl_2$ hydrolysis (Table S1, U7), which is required to initiate Pathway B1 (see Scheme 1).

**DO Consumption from $NHCl_2$ Decomposition.** Once $HNO/NO^-$ forms, DO consumption is required to continue Pathway B1, forming ONOOH (Scheme 1, R5) or $ONOO^-$ (Scheme 1, R4). Therefore, DO should be consumed regardless of DMA presence and serves as an additional $ONOOH/ONOO^-$ (and $HNO/NO^-$) marker. Experiments conducted with ca. 800 $\mu$eq $Cl_2 \cdot L^{-1}$ $NHCl_2$ confirmed that DO consumption occurred at pH 7−10 in the absence of DMA (Figure S8, Supporting Information S2.6). Furthermore, DO profiles tracked with $NHCl_2$ decomposition, indicating that DO consumption was linked to $NHCl_2$ decomposition and supported DO consumption in Pathway B1.

**Peroxynitrite Scavenging Decreased NDMA Formation.** To further support Pathway B1 by (i) providing evidence for $ONOOH/ONOO^-$ formation during $NHCl_2$ decomposition and (ii) showing that NDMA formation proceeded through $ONOOH/ONOO^-$, $ONOOH/ONOO^-$ scavenging experiments were conducted with uric acid. To establish the maximum uric acid concentration that could be used, initial control experiments were conducted with uric acid and $NHCl_2$. Figure S9 (see Supporting Information S2.7) shows the impact of uric acid during $NHCl_2$ decomposition at pH 8−10. Profiles at pH 7 were not provided because of the aforementioned interference with the indophenol method (see Supporting Information S1.3). At pH 9 (Figure S9a,b and Supporting Information S2.7), a detailed uric acid control experiment was conducted to establish the upper uric acid dose, and uric acid doses up to and including 160 $\mu$M had minimal impact on $NHCl_2$ decomposition.

However, a uric acid dose of 200 $\mu$M resulted in greater $NHCl_2$ concentrations that deviated from other data starting at about 0.4 h (Figure S9b). Therefore, a target uric acid dose of about 160 $\mu$M was set as the upper limit and was checked at pH 8 and 10. Uric acid doses of 160 and 170 $\mu$M did not impact $NHCl_2$ decomposition at pH 8 (Figure S9c) and 10 (Figure S9d), respectively. Therefore, Figure 2 shows NDMA yields at uric acid doses of 160 or 170 $\mu$M and less.

Figure 2 shows that uric acid, a $ONOOH/ONOO^-$ scavenger,[30] decreased NDMA formation at pH 7−10. At pH 7, NDMA decreased from about 0.3 $\mu$M to below the limit of quantitation (0.05 $\mu$M) at uric doses of 140 and 170 $\mu$M. This supported that (i) $ONOOH/ONOO^-$ is associated with $NHCl_2$ decomposition and (ii) the vast majority, if not all, of the NDMA formation occurred through a $ONOOH/ONOO^-$ mediated pathway at pH 7. At pH 9, where NDMA formation was maximal, NDMA decreased from about 3.5 to 1.7 $\mu$M as the uric acid dose was increased from 0 to 160 $\mu$M. At pH 10, a

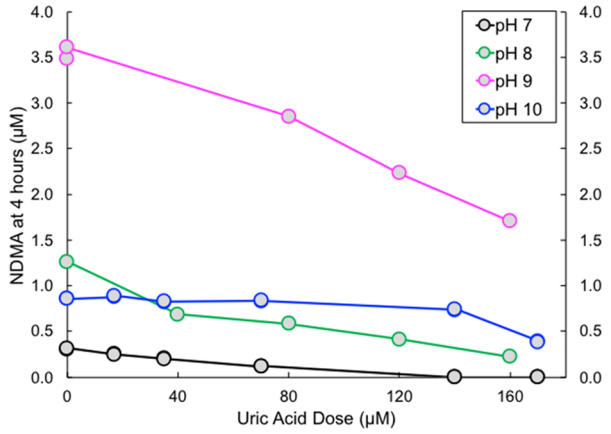


**Figure 2.** NDMA formation at 4 h versus uric acid dose in waters amended with 10 $\mu$M TOTDMA and ca. 800 $\mu$eq $Cl_2 \cdot L^{-1}$ $NHCl_2$ at pH 7, 8, 9, and 10. Uric acid is a known $ONOOH/ONOO^-$ scavenger.[30]

decrease in NDMA formation was observed only after the uric dose was increased from 140 to 170 $\mu$M. On balance, the results in Figure 2 implicated $ONOOH/ONOO^-$ as (i) a downstream product of $NHCl_2$ decomposition and (ii) the central node in NDMA formation during $NHCl_2$ decomposition, supporting Pathway B1 and contradicting Pathway A1. The pH 7 results (Figure 2) support Pathways A2 and B1 over A1 in which all NDMA formation proceeds through $ONOOH/ONOO^-$. This contention is further supported in the remaining subsections.

**NDMA and DMNO Yields from $NHCl_2$ Decomposition.** Further support for $ONOOH/ONOO^-$ formation is NDMA formation concomitantly with DMNO. Experiments conducted with ca. 800 $\mu$eq $Cl_2 \cdot L^{-1}$ $NHCl_2$ and 10 $\mu$M TOTDMA at pH 7−10 showed NDMA and DMNO formation, with DMNO yields of 0.8−1.3% of NDMA regardless of pH (Table S5, Supporting Information S2.8). Masuda et al.[28] and Uppu et al.[32] showed that reactions between $ONOOH/ONOO^-$ and/or their decomposition products with a secondary amine produced *N*-nitrosamines and *N*-nitramines through nitrosation and nitration pathways, respectively. The presence of carbonate has been shown to alter the prevalence of nitrosation and nitration pathways. A study using the precursor morpholine showed that low levels of carbonate relative to $ONOOH/ONOO^-$ could catalyze morpholine nitrosation, but high carbonate levels inhibited nitrosation in favor of *N*-nitramine formation.[32] Because carbonate buffer was used only at pH 10 in this work, experiments were conducted at pH 10 with varying amounts (10−42 mM) of total carbonate ($TOTCO_3$). Results in Table S5 showed that NDMA yields decreased by about a factor of 2 with increasing $TOTCO_3$. DMNO yields also decreased with increasing $TOTCO_3$, but the percentage of DMNO relative to NDMA remained constant (1.1%). The consistent ratios between DMNO and NDMA at pH 7−10 (0.8−1.3%) further support the revision and replacement of Pathway A1 with A2 in which all NDMA formation occurs through $ONOOH/ONOO^-$. Further work is needed to elucidate the role of carbonate species and buffer type relative to the fate of $ONOOH/ONOO^-$ decomposition products during $NHCl_2$ decomposition. However, the decreased NDMA and DMNO yields with increased $TOTCO_3$ suggest a common source, and DMNO formation itself directly implicates $ONOOH/ONOO^-$ formation in Pathway B1.


https://dx.doi.org/10.1021/acs.est.0c06456
Environ. Sci. Technol. 2021, 55, 1740−1749

Table 1. Revised Reactions and Rate Constants Implemented in the UF + RNS Model[j]

| # | reaction stoichiometry[a] | rate expression[a] | rate constant ($M^{-1}\cdot s^{-1}$) unless otherwise noted: published | this work (UF + RNS model) ± SE |
|---|---|---|---|---|
| U7 | $NHCl_2 + H_2O \xrightarrow{k_{u7}} HNO + 2H^+ + 2Cl^-$ | $k_{u7}[NHCl_2][OH^-]$ | [b]110 | 186 ± 6 |
| U8 | $HNO + NHCl_2 \xrightarrow{k_{u8}} HOCl$ + products[c] | $k_{u8}[HNO][NHCl_2]$ | [d]$2.7 \times 10^4$ | $(8.2 \pm 0.8) \times 10^4$ |
| P5 | $NHCl_2 + (CH_3)_2NH \xrightarrow{k_{p5}} (CH_3)_2NNHCl + H^+ + Cl^-$ | $k_{p5}[NHCl_2][(CH_3)_2NH]$ | [e]52 | 28 ± 8 |
| R7 | $ONOOH + (CH_3)_2NH \xrightarrow{k_{r7}} (CH_3)_2NNO$ + products[f] | $k_{r7}[ONOOH][(CH_3)_2NH]$ | NA | [g]$k_{r7} = k_{r7A}\left[\exp\left(-\frac{k_{r7B}}{[H^+]}\right)\right]$; $k_{r7A} = (2.1 \pm 0.4) \times 10^7\ M^{-1}\cdot s^{-1}$; $k_{r7B} = (4.4 \pm 0.3) \times 10^{-10}$ M |
| R8 | $ONOOH + (CH_3)_2NNHCl \xrightarrow{k_{r8}} (CH_3)_2NNO$ + products[h] | $k_{r8}[ONOOH][(CH_3)_2NNHCl]$ | NA | [i]$(1.3 \pm 0.8) \times 10^7$ |

[a]Unidentified intermediate, *I*, of $NHCl_2$ hydrolysis was assumed to be HNO in the UF + RNS model. [b]Jafvert and Valentine.[16] [c]May include $N_2$, $Cl^-$, $H^+$, and other unidentified reaction products. [d]Jafvert and Valentine.[39] [e]Schreiber and Mitch.[10] [f]May include $H_2O_2$[43] and other unidentified reaction products. [g]Empirical formulation currently only applicable at pH 7−10, indicating that ONOOH/$ONOO^-$ decomposition products may also react with $(CH_3)_2NH$ to form NDMA. [h]May include $H^+$, $Cl^-$, $NO_2^-$, and other unidentified reaction products. [i]ONOOH/$ONOO^-$ decomposition products may also react with $(CH_3)_2NNHCl$ to form NDMA. NA: not applicable because these reactions are reported for the first time in this work. [j]Estimated rate constants provided with their standard error (SE, $N$ = 528 total data points). #: reaction number corresponding to Scheme 1; Tables S1−S4 detail published reactions and rate constants

**$NO_2^-$ and $NO_3^-$ Formation from $NHCl_2$ Decomposition.** $NO_2^-$ and $NO_3^-$ form rapidly from ONOOH/$ONOO^-$ decomposition[17] via the reaction of radical species and hydrolysis, respectively. Therefore, $NO_2^-$ and $NO_3^-$ are markers for ONOOH/$ONOO^-$ formation. As noted in the Supporting Information S1.4 and S2.9, it was only possible to accurately quantify $NO_2^-$ and $NO_3^-$ after $NHCl_2$ had decomposed to less than about 50 $\mu$eq $Cl_2\cdot L^{-1}$ because of a positive interference produced on $NO_2^-$ by the quenching of $NHCl_2$ with thiosulfate. Figure S10 shows that quenching 50 $\mu$eq $Cl_2\cdot L^{-1}$ $NHCl_2$ produced about 1 $\mu$M-N $NO_2^-$. Therefore, $NO_2^-$ and $NO_3^-$ are reported in Table S6 (Supporting Information S2.9) as yields only at pH 8−10 in the absence and presence of 10 $\mu$M TOTDMA. Without TOTDMA, $NO_2^-$ production was greater at pH 10 (26 $\mu$M) compared to pH 8 and 9 (both 10 $\mu$M) and $NO_3^-$ production was similar at all three pH levels (14−16 $\mu$M); therefore, the percentage of $NO_2^-$ relative to $NO_2^-$ plus $NO_3^-$ increased with pH, in agreement with the ONOOH/$ONOO^-$ reaction scheme validated by Kirsch et al.,[17] albeit at 37 °C (e.g., internal temperature of the human body). The addition of 10 $\mu$M TOTDMA resulted in decreased sums of $NO_2^-$ plus $NO_3^-$ (Table S6) by 8 $\mu$M at pH 8, 14 $\mu$M at pH 9, and 6 $\mu$M at pH 10. These decreases are consistent with the ONOOH/$ONOO^-$ conversion to other intermediates and minor end products, including NDMA (see Scheme 1) that is maximal at pH 9 (see Figure 1). The DO formation from the production of $NO_2^-$ is detailed in the Supporting Information (S2.10, see also Table S7).

**UF + RNS Model Implementation.** To assess the RNS-mediated NDMA formation pathways (see Scheme 1, B1 and A2) and to help interpret the experimental data, a kinetic model (UF + RNS) was implemented in AQUASIM.[36] The UF + RNS model included the UF model[16] (Table S1, U1−U14), assuming that HNO was *I* formed by $NHCl_2$ hydrolysis (U7); the two previously described RNS-related pathways, B1 and A2; and the Kirsch et al.[17] model for ONOOH/$ONOO^-$ decomposition to $NO_2^-$ and $NO_3^-$. Table S8 (see S2.11) shows that the current AQUASIM implementation of the Kirsch et al.[17] model was within 0.1−3.5% of their digitized $NO_2^-$ and $NO_3^-$ concentrations between pH 7 and 10. Pathway A2 was included in lieu of Pathway A1 from the UF + SM model. Subsequently, the implemented UF + RNS model was used along with the experimental data (see Supporting Information S2.11, Table S9) to estimate revisions to three existing ($k_{u7}$, $k_{u8}$, and $k_{p5}$) and three new ($k_{r7A}$, $k_{r7B}$, and $k_{r8}$) parameters implemented in the UF + RNS model (Table 1).

Rate constants for U7−U10 were empirical in the UF model,[16] formulated to match chloramine species concentrations only; therefore, they were initially all considered for re-estimation in the current work. Preliminary analysis indicated that $k_{u9}$ and $k_{u10}$ were not sensitive to the conditions of this study (i.e., preformed $NHCl_2$); therefore, $k_{u9}$ and $k_{u10}$ were excluded from the final parameter estimation procedure. Table 1 shows the revised rate constants ± 1 standard error for $k_{u7}$ (from 110 to 186 ± 6 $M^{-1}\cdot s^{-1}$) and $k_{u8}$ (from $2.7 \times 10^4$ to $(8.2 \pm 0.8) \times 10^4\ M^{-1}\cdot s^{-1}$).

R7 was included in the UF + RNS model as a new NDMA-formation reaction between ONOOH and DMA (Scheme 1, Pathway B1), justified by (i) the scavenger results (Figure 2) that indicated that ONOOH/$ONOO^-$ was a central node in NDMA formation and (ii) the RNS literature that showed that ONOOH/$ONOO^-$ and/or their decomposition products (i.e., radicals) reacted with DMA to form NDMA.[28] Figure 1 indicated that NDMA formation was maximal at pH 9, which is close to the average of the p$K_a$ values listed in Table S3 for ONOOH/$ONOO^-$ (p$K_a$ = 6.8) and $DMAH^+$/DMA (p$K_a$ = 10.73). Generally, the reaction rate between an acid of one species and conjugate base of another is maximal at a pH equal to the average of their p$K_a$ values, which is pH 8.8 in this case. The UF + SM model used DMA (i.e., the uncharged base form) in the NDMA formation pathway.[10] Therefore, if a direct reaction occurred involving DMA (base form), ONOOH (acid form) is the likely candidate. The estimated rate constant for R7 (see Table 1 and Table S11) was determined to be acid catalyzed, $k_{r7} = k_{r7A}\left[\exp\left(-\frac{k_{r7B}}{[H^+]}\right)\right]$ with $k_{r7A} = (2.1 \pm 0.4) \times 10^7\ M^{-1}\cdot s^{-1}$ and $k_{r7B} = (4.4 \pm 0.3) \times 10^{-10}$ M, an empirical formulation that warrants a future research effort to further develop a mechanistic revision of the UF + RNS model.

Although our NDMA data could also be simulated by a UF + RNS model version using only Pathways A1 (e.g., the UF +



https://dx.doi.org/10.1021/acs.est.0c06456
Environ. Sci. Technol. 2021, 55, 1740−1749

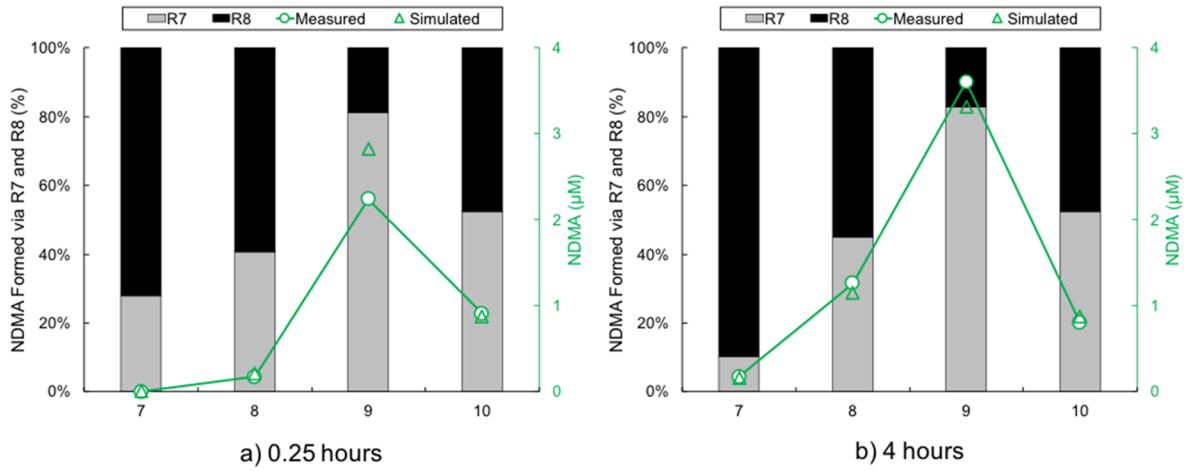


**Figure 3.** Percentage of UF + RNS model simulated NDMA formed via R7 and R8 (primary *y* axis) and measured and UF + RNS model simulated NDMA concentrations (secondary *y* axis) at pH 7, 8, 9, and 10 at (a) 0.25 h and (b) 4 h.

SM model) and B1, our experimental data did not support Pathway A1 because NDMA formation was shut down at pH 7 in the ONOOH/$ONOO^-$ scavenging experiments (Figure 2). Therefore, Pathway A1 was revised and Reaction P8 (UDMH-Cl + DO) was the likely candidate for this revision because it is spin-forbidden and DO consumption was not previously kinetically validated.[10] This prompted the assessment of Pathway A2 in which P8 was replaced by R8, the reaction of UDMH-Cl and ONOOH to form NDMA with an estimated rate constant of $(1.3 \pm 0.8) \times 10^7$ $M^{-1}{\cdot}s^{-1}$ (Table 1, $k_{r8}$). The current implementation of R8 is also empirical because it is not known if it is a direct reaction with ONOOH/$ONOO^-$ and/or their decomposition products,[32] but it was assumed that either could be simulated based on the ONOOH concentration. Rate constants for reactions P5 and P7 were also initially considered for revision, but P7 proved insensitive and was therefore not re-estimated. The final parameter estimation resulted in a decreased rate constant estimate for P5 from 52 to $28 \pm 8$ $M^{-1}{\cdot}s^{-1}$, a logical result given that the UF + SM model did not consider Pathway B1.

**UF + RNS Model Well Simulated $NHCl_2$, $NH_2Cl$, DO, and NDMA at pH 7−10.** The revised rate constants for U7 and U8 were validated by comparing simulated UF + RNS and UF model free chlorine, $NH_2Cl$, and $NHCl_2$ concentrations for 20 additional experimental conditions (Exp. 1−15 and 23−27) from Jafvert[38] that are shown in Figures S11−S14, S16d, and S17 (see Supporting Information S2.12 and Table S12 for WRSS and average WRSS (AWRSS) comparisons). In addition, the $NH_2Cl$ and $NHCl_2$ data sets used in parameter estimation (Table S9) are also included in Table S12. Compared to the UF model, the simulated free chlorine, $NH_2Cl$, and $NHCl_2$ concentrations with the UF + RNS model had similar or lower summed totals of WRSS and AWRSS (see Table S12), indicating that the UF + RNS model simulated these data comparably to the UF model. These results showed that the revised estimates to the rate constants for U7 and U8 in the UF + RNS model did not compromise the simulations of chloramine species concentrations over a wide range of conditions.

Figure 1 shows the UF + RNS model simulations and measured time-course profiles of DO and NDMA at pH 7−10. The kinetics and yields of these measured data were well simulated by the UF + RNS model at all pH levels tested. Notably, at pH 9 and 10 (Figure 1c,d), the simulated DO and NDMA profiles matched the measured data in terms of kinetics and yields throughout the 4 h time-course.

The UF + RNS model was used to determine the relative importance of the two NDMA formation pathways (i.e., Pathways A2 and B1). Figure 3 summarizes the percentage of the simulated NDMA that formed via R7 (DMA + ONOOH, Pathway B1) and R8 (UDMH-Cl + ONOOH, Pathway A2) at 0.25 h (Figure 3a) and 4 h (Figure 3b) along with the UF + RNS model simulated and measured NDMA concentrations.

At pH 7, R8 was the predominate NDMA formation pathway (70−90%), although the measured NDMA was lower at pH 7 compared to the other pH levels. At pH 8, R8 accounted for 55−59% of the NDMA formation, illustrating that Pathways A2 and B1 were both important contributors. At pH 9, where NDMA formation was maximal, R7 was the predominant NDMA formation pathway at 0.25 and 4 h (81−83%). At pH 10, R7 accounted for 52% of the NDMA formation at 0.25 and 4 h, illustrating the importance of the A2 and B1 pathways. The results in Figures 1 and 3 support the UF + RNS model because it captured the kinetics and yields of the measured DO and NDMA profiles. Pathway B1 (see Scheme 1) was important at pH 7−10 and, together with Pathway A2, indicated that all the measured NDMA could be accounted for through ONOOH/$ONOO^-$, stemming from $NHCl_2$ decomposition.

**Current UF + RNS Model Limitations and Future Research Needs.** The UF + RNS model Pathways B1 and A2 each currently use an empirical NDMA formation reaction, R7 and R8, respectively. Because of the complexity of the current reaction scheme, the mechanistic determination of R7 and R8 is beyond the scope of the current research and is an avenue of future research. Potential cross-interactions remain to be investigated between the chloramine species and known decomposition products of ONOOH/$ONOO^-$, including hydrogen peroxide and hydroxyl radical.[44,45] In addition, deviations between the measured $NO_2^-$ and $NO_3^-$ formation and UF + RNS model simulated values (see Table S13 in Supporting Information S2.13) indicate the need for kinetic $N_2$, $NO_2^-$, and $NO_3^-$ data to validate and/or revise the Kirsch et al.[17] ONOOH/$ONOO^-$ decomposition model for drinking water conditions and temperatures. Finally, the UF + RNS model overpredicted the $N_2O$ data at pH 10 (Figure 1d) but


https://dx.doi.org/10.1021/acs.est.0c06456
Environ. Sci. Technol. 2021, 55, 1740−1749

underpredicted $N_2O$ at pH 7 to 9 (Figure 1a–c), with the corresponding WRSS and AWRSS shown in Table S10, illustrating the need to measure $N_2$, $NO_2^-$, and $NO_3^-$ kinetically in future work to facilitate further advancement of the UF + RNS model.

**Mechanistic Considerations.** This study presented multiple lines of evidence to demonstrate that $NHCl_2$ hydrolysis resulted in HNO formation (Scheme 1, U7), the so-called unidentified reactive intermediate (*I*) in the UF model.[16] Per Pathway B1, $HNO/NO^-$ reacts through three competing pathways, which include two minor pathways: (i) $N_2O$ formation (see Figure 1) via R1 and/or R2 → R3 and (ii) reaction with DO (see Figure 1) to form $ONOOH/ONOO^-$ via R5 and/or R2 → R4, and one major pathway: (iii) $N_2$ formation via U8–U10 that has been previously quantified during $NH_2Cl$ decomposition[40] and can now be used to investigate nitrogen mass balances during $NHCl_2$ decomposition along with the advancements made in this work.

The two minor pathways are important new additions to $NHCl_2$ decomposition chemistry because they help explain the formation of $NO_2^-$, $NO_3^-$, NDMA, and DMNO. Table S13 shows that the measured values for $N_2O$, $NO_2^-$, and $NO_3^-$ account for ca. 4–6% of the nitrogen originally present in $NHCl_2$ and total free ammonia ($NH_3$ + $NH_4^+$). Although complete nitrogen mass balances have not been tracked during $NHCl_2$ decomposition, Saunier[46] estimated that $NO_3^-$ yields accounted for 8–11% of the total nitrogen. Future work should include $N_2$, $NO_2^-$, $NO_3^-$, and total free ammonia kinetic measurements along with the products kinetically measured in this study.

Measurements of $NHCl_2$, $NH_2Cl$, $N_2O$, DO, $NO_2^-$, $NO_3^-$, NDMA, and DMNO implicate $ONOOH/ONOO^-$ as a proposed unstable intermediate formed during $NHCl_2$ decomposition, which was supported by experiments with uric acid, a $ONOOH/ONOO^-$ scavenger.[30] NDMA decreased with increasing uric acid at pH 7–10 (Figure 2), and the shutdown of NDMA formation at pH 7 spurred the replacement of P8 in the UF + SM model with R8 in the UF + RNS model (Table 1), corresponding to the replacement of Pathway A1 with A2 in Scheme 1. Together with R7, the UF + RNS model accurately captured the kinetics and yields of DO and NDMA at pH 7–10 (Figure 1), indicating that all NDMA formation (Figure 3) could be accounted for through $ONOOH/ONOO^-$ formation, stemming from $NHCl_2$ decomposition.

**Implications.** A logical extension of the current results is that scavenging $HNO/NO^-$ and/or $ONOOH/ONOO^-$ may curb NDMA formation in chloramine systems. $NHCl_2$ does not accumulate to measurable concentrations at pH 9 and greater because its rate of decomposition is greater than its formation,[16] but if total free ammonia is in excess as is the case in chloramine systems, chloramine decomposition occurs through $NHCl_2$; therefore, $HNO/NO^-$ and $ONOOH/ONOO^-$ will form regardless of the pH. Scavenging of these RNS and/or strategies to promote chloramine stability would presumably lead to less NDMA formation.

Future research should extend the UF + RNS model presented here. Specifically, a further mechanistic revision of the UF + RNS model is needed, focusing on U7–U10,[16] R7, R8, and $ONOOH/ONOO^-$ decomposition chemistry[17] to well simulate the measured profiles of the minor products ($N_2O$, $NO_2^-$, $NO_3^-$) and the major products ($N_2$ and total free ammonia) while maintaining simulations of chloramine species (Figures S4, S7, S15, and S16), DO (Figure 1), and NDMA (Figure 1).

Further experimental work should consider additional $HNO/NO^-$ formation pathways independent of $NHCl_2$, including the reaction between $NH_2Cl$ and hydroxylamine ($NH_2OH$) generated from ammonia-oxidizing bacteria.[25,47] The reaction of $NH_2Cl$ with $NH_2OH$ implicated $HNO/NO^-$ and $ONOOH/ONOO^-$ production,[25] providing a potential mechanism to evaluate and potentially explain the enhanced NDMA formation observed during nitrification episodes.[48]

## ■ ASSOCIATED CONTENT

### Supporting Information

The Supporting Information is available free of charge at https://pubs.acs.org/doi/10.1021/acs.est.0c06456.

Chloramine preparation and quantification, nitrite, nitrate, NDMA, and DMNO quantification, kinetic evaluation of Pathway A1, applicability of the unified model for chloramine profiles, dissolved oxygen formation from nitrite production, UF + RNS model rate constants and goodness of fit measures, and impact of uric acid on $NHCl_2$ decomposition (PDF)

## ■ AUTHOR INFORMATION


### Corresponding Author

**Julian L. Fairey** − *Department of Civil Engineering, University of Arkansas, Fayetteville, Arkansas 72701, United States;* orcid.org/0000-0003-3129-3929; Phone: (479) 575-4023; Email: julianf@uark.edu

### Authors

**Huong T. Pham** − *Department of Civil Engineering, University of Arkansas, Fayetteville, Arkansas 72701, United States*

**David G. Wahman** − *U.S. Environmental Protection Agency, Cincinnati, Ohio 45268, United States;* orcid.org/0000-0002-0167-8468

Complete contact information is available at: https://pubs.acs.org/10.1021/acs.est.0c06456


### Notes

The authors declare no competing financial interest.

## ■ ACKNOWLEDGMENTS

This work was supported by National Science Foundation Award Numbers 1604820 and 2034481 and an Arkansas Water Resources Center student grant. The authors acknowledge Michael Elovitz (EPA, Cincinnati OH) and three anonymous peer reviewers for helpful comments on previous drafts of this manuscript. Research was not performed or funded by EPA and was not subject to EPA's quality system requirements. Views expressed are those of the authors and do not necessarily represent views or policies of EPA.

## ■ REFERENCES

(1) Cornwell Engineering Group. *Water Utility Disinfection Survey Report*; American Water Works Association, 2018.

(2) Russell, C. G.; Blute, N. K.; Via, S.; Wu, X.; Chowdhury, Z. Nationwide assessment of nitrosamine occurrence and trends. *J. - Am. Water Works Assoc.* **2012**, *104*, E205–E217.

(3) Hrudey, S. E.; Charrois, J. W. A., *Disinfection By-Products and Human Health*. IWA Publishing and Australian Water Association: London, 2012; p 304.

(4) Lide, D. R. *CRC Handbook of Chemistry and Physics*. Taylor & Francis: 2010-2011; Vol. 91st Edition.
(5) Shen, R.; Andrews, S. A. Demonstration of 20 pharmaceuticals and personal care products (PPCPs) as nitrosamine precursors during chloramine disinfection. *Water Res.* **2011**, *45*, 944−952.
(6) Leavey-Roback, S. L.; Krasner, S. W.; Suffet, I. M. Veterinary antibiotics used in animal agriculture as NDMA precursors. *Chemosphere* **2016**, *164*, 330−338.
(7) Flowers, R. C.; Singer, P. C. Anion Exchange Resins as a Source of Nitrosamines and Nitrosamine Precursors. *Environ. Sci. Technol.* **2013**, *47*, 7365−7372.
(8) Morran, J.; Whittle, M.; Fabris, R. B.; Harris, M.; Leach, J. S.; Newcombe, G.; Drikas, M. Nitrosamines from pipeline materials in drinking water distribution systems. *J. - Am. Water Works Assoc.* **2011**, *103*, 76.
(9) Choi, J.; Valentine, R. L. Formation of N-nitrosodimethylamine (NDMA) from reaction of monochloramine: A new disinfection by-product. *Water Res.* **2002**, *36*, 817−824.
(10) Schreiber, I. M.; Mitch, W. A. Nitrosamine Formation Pathway Revisited: The Importance of Chloramine Speciation and Dissolved Oxygen. *Environ. Sci. Technol.* **2006**, *40*, 6007−6014.
(11) Spahr, S.; Cirpka, O. A.; von Gunten, U.; Hofstetter, T. B. Formation of N-Nitrosodimethylamine during Chloramination of Secondary and Tertiary Amines: Role of Molecular Oxygen and Radical Intermediates. *Environ. Sci. Technol.* **2017**, *51*, 280−290.
(12) Le Roux, J.; Gallard, H.; Croué, J.-P. Chloramination of nitrogenous contaminants (pharmaceuticals and pesticides): NDMA and halogenated DBPs formation. *Water Res.* **2011**, *45*, 3164−3174.
(13) Choi, J.; Valentine, R. L. A kinetic model of N-nitrosodimethylamine (NDMA) formation during water chlorination/chloramination. *Water Sci. Technol.* **2002**, *46*, 65−71.
(14) Mitch, W. A.; Sedlak, D. L. Formation of N-nitrosodimethylamine (NDMA) from dimethylamine during chlorination. *Environ. Sci. Technol.* **2002**, *36*, 588−595.
(15) Yagil, G.; Anbar, M. The Kinetics of Hydrazine Formation from Chloramine and Ammonia. *J. Am. Chem. Soc.* **1962**, *84*, 1797−1803.
(16) Jafvert, C. T.; Valentine, R. L. Reaction Scheme for the Chlorination of Ammoniacal Water. *Environ. Sci. Technol.* **1992**, *26*, 577−586.
(17) Kirsch, M.; Korth, H. G.; Wensing, A.; Sustmann, R.; de Groot, H. Product Formation and Kinetic Simulations in the pH Range 1-14 Account for a Free-Radical Mechanism of Peroxynitrite Decomposition. *Arch. Biochem. Biophys.* **2003**, *418*, 133−150.
(18) Schreiber, I. M.; Mitch, W. A. Influence of the Order of Reagent Addition on NDMA Formation During Chloramination. *Environ. Sci. Technol.* **2005**, *39*, 3811−3818.
(19) Krasner, S. W.; Mitch, W. A.; McCurry, D. L.; Hanigan, D.; Westerhoff, P. Formation, precursors, control, and occurrence of nitrosamines in drinking water: A review. *Water Res.* **2013**, *47*, 4433−4450.
(20) Huang, M. E.; Huang, S.; McCurry, D. L. Re-Examining the Role of Dichloramine in High-Yield N-Nitrosodimethylamine Formation from N,N-Dimethyl-$\alpha$-arylamines. *Environ. Sci. Technol. Lett.* **2018**, *5*, 154−159.
(21) Selbes, M.; Kim, D.; Ates, N.; Karanfil, T. The roles of tertiary amine structure, background organic matter and chloramine species on NDMA formation. *Water Res.* **2013**, *47*, 945−953.
(22) Wei, I. W. Chlorine-Ammonia Breakpoint Reactions: Kinetics and Mechanism; Ph.D. Dissertation, Harvard University: Cambridge, MA, 1972, 229 Pages.
(23) Shafirovich, V.; Lymar, S. V. Spin-Forbidden Deprotonation of Aqueous Nitroxyl (HNO). *J. Am. Chem. Soc.* **2003**, *125*, 6547−6552.
(24) Shafirovich, V.; Lymar, S. V. Nitroxyl and its Anion in Aqueous Solutions: Spin States, Protic Equilibria, and Reactivities Toward Oxygen and Nitric Oxide. *Proc. Natl. Acad. Sci. U. S. A.* **2002**, *99*, 7340−7345.
(25) Wahman, D. G.; Speitel, G. E., Jr.; Machavaram, M. V. A Proposed Abiotic Reaction Scheme for Hydroxylamine and Monochloramine under Chloramination Relevant Drinking Water Conditions. *Water Res.* **2014**, *60*, 218−227.
(26) Smulik, R.; Dębski, D.; Zielonka, J.; Michałowski, B.; Adamus, J.; Marcinek, A.; Kalyanaraman, B.; Sikora, A. Nitroxyl (HNO) Reacts with Molecular Oxygen and Forms Peroxynitrite at Physiological pH: Biological Implications. *J. Biol. Chem.* **2014**, *289*, 35570−35581.
(27) Hamer, M.; Morales Vasquez, M. A.; Doctorovich, F. HNO: Redox Chemistry and Interactions with small inorganic molecules. In *The Chemistry and Biology of Nitroxyl (HNO)*; Doctorovich, F.; Farmer, P. J.; Marti, M., Eds. Elsevier, 2016.
(28) Masuda, M.; Mower, H. F.; Pignatelli, B.; Celan, I.; Friesen, M. D.; Nishino, H.; Ohshima, H. Formation of N-nitrosamines and N-nitramines by the reaction of secondary amines with peroxynitrite and other reactive nitrogen species: Comparison with nitrotyrosine formation. *Chem. Res. Toxicol.* **2000**, *13*, 301−308.
(29) Pliss, G. B.; Zabezhinski, M. A.; Petrov, A. S.; Khudoley, V. V. Peculiarities of N-Nitramines carcinogenic action. *Arch. Geschwulstforsch.* **1982**, *52*, 629−634.
(30) Hooper, D. C.; Spitsin, S.; Kean, R. B.; Champion, J. M.; Dickson, G. M.; Chaudhry, I.; Koprowski, H. Uric acid, a natural scavenger of peroxynitrite, in experimental allergic encephalomyelitis and multiple sclerosis. *Proc. Natl. Acad. Sci. U. S. A.* **1998**, *95*, 675−680.
(31) Squadrito, G. L.; Cueto, R.; Splenser, A. E.; Valavanidis, A.; Zhang, H.; Uppu, R. M.; Pryor, W. A. Reaction of Uric Acid with Peroxynitrite and Implications for the Mechanism of Neuroprotection by Uric Acid. *Arch. Biochem. Biophys.* **2000**, *376*, 333−337.
(32) Uppu, R. M.; Squadrito, G. L.; Bolzan, R. M.; Pryor, W. A. Nitration and Nitrosation by Peroxynitrite: Role of CO2 and Evidence for Common Intermediates. *J. Am. Chem. Soc.* **2000**, *122*, 6911−6916.
(33) Do, T. D.; Chimka, J. R.; Fairey, J. L. Improved (and Singular) Disinfectant Protocol for Indirectly Assessing Organic Precursor Concentrations of Trihalomethanes and Dihaloacetonitriles. *Environ. Sci. Technol.* **2015**, *49*, 9858−9865.
(34) Padhye, L.; Luzinova, Y.; Cho, M.; Mizaikoff, B.; Kim, J.-H.; Huang, C.-H. PolyDADMAC and Dimethylamine as Precursors of N-Nitrosodimethylamine during Ozonation: Reaction Kinetics and Mechanisms. *Environ. Sci. Technol.* **2011**, *45*, 4353−4359.
(35) Shen, R.; Andrews, S. A. Formation of NDMA from ranitidine and sumatriptan: The role of pH. *Water Res.* **2013**, *47*, 802−810.
(36) Reichert, P. AQUASIM - A tool for simulation and data analysis of aquatic systems. *Water Sci. Technol.* **1994**, *30*, 21−30.
(37) Draper, N. R.; Smith, H. *Applied Regression Analysis*; John Wiley & Sons, Inc.: New York, 1998.
(38) Jafvert, C. T.. *A Unified Chlorine-Ammonia Speciation and Fate Model*; PhD Dissertation, PhD, University of Iowa, 1985, 222 Pages.
(39) Jafvert, C. T.; Valentine, R. L. Dichloramine Decomposition in the Presence of Excess Ammonia. *Water Res.* **1987**, *21*, 967−973.
(40) Vikesland, P. J.; Ozekin, K.; Valentine, R. L. Effect of natural organic matter on monochloramine decomposition: Pathway elucidation through the use of mass and redox balances. *Environ. Sci. Technol.* **1998**, *32*, 1409−1416.
(41) *Chemicalize* available at: https://chemicalize.com/welcome, ChemAxon, Accessed on: December 20, 2020.
(42) Irvine, J. C.; Ritchie, R. H.; Favaloro, J. L.; Andrews, K. L.; Widdop, R. E.; Kemp-Harper, B. K. Nitroxyl (HNO): the Cinderella of the nitric oxide story. *Trends Pharmacol. Sci.* **2008**, *29*, 601−608.
(43) Kirsch, M.; Lomonosova, E. E.; Korth, H. G.; Sustmann, R.; de Groot, H. Hydrogen peroxide formation by reaction of peroxynitrite with HEPES and related tertiary amines - Implications for a general mechanism. *J. Biol. Chem.* **1998**, *273*, 12716−12724.
(44) McKay, G.; Sjelin, B.; Chagnon, M.; Ishida, K. P.; Mezyk, S. P. Kinetic study of the reactions between chloramine disinfectants and hydrogen peroxide: Temperature dependence and reaction mechanism. *Chemosphere* **2013**, *92*, 1417−1422.
(45) Gleason, J. M.; McKay, G.; Ishida, K. P.; Mezyk, S. P. Temperature dependence of hydroxyl radical reactions with chloramine species in aqueous solution. *Chemosphere* **2017**, *187*, 123−129.


https://dx.doi.org/10.1021/acs.est.0c06456
*Environ. Sci. Technol.* 2021, 55, 1740−1749

(46) Saunier, B. M. Kinetics of Breakpoint Chlorination and Disinfection; Ph.D. Dissertation, University of California, Berkeley, CA, 1976, 370 Pages.
(47) Wahman, D. G.; Speitel, G. E., Jr. Hydroxylamine addition impact to Nitrosomonas europaea activity in the presence of monochloramine. *Water Res.* **2015**, *68*, 719−730.
(48) Zeng, T.; Mitch, W. A. Impact of Nitrification on the Formation of *N*-Nitrosamines and Halogenated Disinfection By-products within Distribution System Storage Facilities. *Environ. Sci. Technol.* **2016**, *50*, 2964−2973.



https://dx.doi.org/10.1021/acs.est.0c06456
*Environ. Sci. Technol.* 2021, 55, 1740−1749